Biochemical Pharmacology 78 (2009) 1456–1463

Contents lists available at ScienceDirect

Biochemical Pharmacology

journal homepage: www.elsevier.com/locate/biochempharm

Useful pharmacological parameters for G-protein-coupled receptor homodimers obtained from competition experiments. Agonist–antagonist binding modulation

Vicent Casadó, Carla Ferrada, Jordi Bonaventura, Eduard Gracia, Josefa Mallol, Enric I. Canela *, Carmen Lluís, Antoni Cortés, Rafael Franco

Institut d'Investigacions Biomèdiques August Pi i Sunyer, Centro de Investigación Biomédica en Red sobre Enfermedades Neurodegenerativas (CIBERNED), Department of Biochemistry and Molecular Biology, Faculty of Biology, University of Barcelona, Avda. Diagonal 465, 08028 Barcelona, Spain

ARTICLE INFO

Article history:
Received 14 May 2009
Received in revised form 16 July 2009
Accepted 20 July 2009

Keywords:
Adenosine receptors
Dopamine receptors
Competition curves
Two-state dimer receptor model
Equilibrium dissociation constants
Cooperativity

ABSTRACT

Many G-protein-coupled receptors (GPCRs) are expressed on the plasma membrane as dimers. Since drug binding data are currently fitted using equations developed for monomeric receptors, the interpretation of the pharmacological data are equivocal in many cases. As reported here, GPCR dimer models account for changes in competition curve shape as a function of the radioligand concentration used, something that cannot be explained by monomeric receptor models. Macroscopic equilibrium dissociation constants for the agonist and homotropic cooperativity index reflecting the intramolecular communication within the dopamine D_1 or adenosine A_{2A} receptor homodimer as well as hybrid equilibrium dissociation constant, which reflects the antagonist/agonist modulation may be calculated by fitting binding data from antagonist/agonist competition experiments to equations developed from dimer receptor models. Comparing fitting the data by assuming a classical monomeric receptor model or a dimer model, it is shown that dimer receptor models provide more clues useful in drug discovery than monomer-based models.

1. Introduction

Knowing the binding affinity of newly developed drugs is a mandatory step for the pharmacological characterization of drugs acting on their targets. Quite often, displaying data on the binding of natural or synthetic neurotransmitters or neuromodulators to specific G-protein-coupled receptors (GPCRs) gives concave upward Scatchard plots [1] rather than a straight line, reflecting cooperativity in the binding. The approach most often used to deal with such type of data is based on two assumptions: one is that receptors are monomeric and another is that two different (monomeric) receptor forms are capable of binding the ligand but with different affinities. In its most commonly used form, it is assumed that one population of receptors is coupled to a G-protein and displays high-affinity, whereas another is uncoupled from any G-protein and displays low-affinity binding for agonists. These two different forms of the receptor, which have different affinities for agonists (K_{DH} and K_{DL}), have to be independent and cannot be in equilibrium. For this reason, the model is usually known as the two-independent-site model [2]. The two-independent-site approach has been very useful and has been often used in cases of complex binding. However this approach is meaningful only if the two states of the receptor with high- and low-affinity for ligands are totally independent, i.e. they are not in equilibrium and they cannot be converted into each other. This is possible in artificial systems such as that described by Whorton et al. [3] but there is evidence that it is not likely to happen in cells.

Given the predominance of heptaspanning membrane receptors as dimers (see [4–15] for an extensive review), the interpretation of complex binding using a receptor dimer model might be more straightforward. In this case positive or negative cooperativity is naturally explained by assuming, like in the case of the enzymes, that binding of the first ligand to the dimer modifies the equilibrium parameters of binding of the second ligand molecule to the dimer. Based on the above considerations dimer receptor models have been developed by some authors [1,16–19]. Dimer models are able to explain both concave upward and concave downward Scatchard plots that likely express, respectively, negative and positive cooperativity. One relevant feature of the two-state dimer model reported by Franco et al. [1,17] is the possibility of calculating the degree of cooperativity among protomers.

* Corresponding author. Tel.: +34 934021211; fax: +34 934021559.
E-mail addresses: vcasado@ub.edu (V. Casadó), cferradam@gmail.com (C. Ferrada), jorgh82@gmail.com (J. Bonaventura), edugss@gmail.com (E. Gracia), jmallol@ub.edu (J. Mallol), ecanela@ub.edu (E.I. Canela), clluis@ub.edu (C. Lluís), antonicortes@ub.edu (A. Cortés), rfranco@ub.edu (R. Franco).

0006-2952/$ – see front matter © 2009 Published by Elsevier Inc.
doi:10.1016/j.bcp.2009.07.012

Although from a theoretical point of view it seems obvious that dimer models will be of election for fitting binding data to a great number of GPCRs, dimer models, as originally described [1,17,18], provided equations including microscopic binding constants that did not give practical information about how to determine the macroscopic constants values. The recent development by Casadó et al. [19] describes a macroscopic analysis that is readily applicable in day to day receptor pharmacological data management. In this paper D_1 dopamine and A_{2A} adenosine receptors were selected as a model due to their well established ability to form homodimers [20–23]. Ligand binding data from antagonist/agonist competition experiments were fitted to equations developed from the two-independent-site model for monomeric receptors or from the two-state dimer receptor model. The macroscopic equilibrium dissociation constants for the agonist, the dimer cooperativity index reflecting the molecular communication within the dimer for the agonist binding and a hybrid equilibrium radioligand/competitor dissociation constant, which reflects the antagonist/agonist modulation in competition experiments, were calculated. These parameters may help in the criteria for selecting drugs under development.

2. Materials and methods

2.1. Membrane preparation and protein determination

Membrane suspensions from sheep brain striatum were processed as described previously [2,24]. Tissue was disrupted with a Polytron homogenizer (PTA 20 TS rotor, setting 3; Kinematica, Basel, Switzerland) for three 5 s-periods in 10 volumes of 50 mM Tris–HCl buffer, pH 7.4 containing a proteinase inhibitor cocktail (Sigma, St. Louis, MO, USA). Cell debris were eliminated and membranes were obtained by centrifugation at 105,000 × *g* (40 min, 4 °C), and the pellet was resuspended and recentrifuged under the same conditions. The pellet was stored at −80 °C and was washed once more as described above and resuspended in 50 mM Tris–HCl buffer for immediate use. Protein was quantified by the bicinchoninic acid method (Pierce Chemical Co., Rockford, IL, USA) using bovine serum albumin dilutions as standard.

2.2. Radioligand binding experiments

Membrane suspensions (0.25–0.5 mg protein/ml) were incubated 2 h at 25 °C in 50 mM Tris–HCl buffer, pH 7.4, containing 10 mM $MgCl_2$ and 2 U/ml adenosine deaminase (EC 3.5.4.4; Roche, Basel, Switzerland; only in A2A receptor binding experiments) with the indicated free concentration of the dopamine D_1 receptor antagonist [^{3}H]SCH 23390 (NEN PerkinElmer, Wellesley, MA, USA) or with 0.7 or 3.6 nM free concentration of the adenosine A_{2A} receptor antagonist [^{3}H]ZM 241385 (American Radiolabelled Chemicals, St. Louis, MO, USA) and increasing concentrations of, respectively, the D_1 receptor agonist SKF 81297 or SKF 38393 (triplicates of 13 different concentrations from 0.1 nM to 50 μM; Tocris, Ellisville, MO, USA) or increasing concentrations of the A_{2A} receptor agonist CGS 21680 (triplicates of 13 different concentrations from 0.1 nM to 50 μM; Tocris, Ellisville, MO, USA) respectively. Nonspecific binding was determined in the presence of 10 μM SCH 23390 or 10 μM ZM 241385 (Tocris, Ellisville, MO, USA) and confirmed that the value was the same as calculated by extrapolation of the competition curves. Free and membrane-bound ligand were separated by rapid filtration of 500 μl aliquots in a cell harvester (Brandel, Gaithersburg, MD, USA) through Whatman GF/C filters embedded in 0.3% polyethylenimine that were subsequently washed for 5 s with 5 ml of ice-cold Tris–HCl buffer. The filters were incubated with 10 ml of Ecoscint H scintillation cocktail (National Diagnostics, Atlanta, GA, USA) overnight at room temperature and radioactivity counts were determined using a Tri-Carb 1600 scintillation counter (PerkinElmer, Boston, MA, USA) with an efficiency of 62% [24].

2.3. Binding data analysis

Radioligand competition curves were analyzed by nonlinear regression using the commercial Grafit curve-fitting software (Erithacus Software, Surrey, UK), by fitting the specific binding data to the two-state dimer receptor model [1,17]. To calculate the macroscopic equilibrium dissociation constants involved in the binding of the agonist, the following equation for a competition binding experiment deduced by Casadó et al. [19] was considered:

$$A_{bound} = \frac{(K_{DA2}A + 2A^2 + K_{DA2}AB/K_{DAB})R_T}{K_{DA1}K_{DA2} + K_{DA2}A + A^2 + K_{DA2}AB/K_{DAB} + K_{DA1}K_{DA2}B/K_{DB1} + K_{DA1}K_{DA2}B^2/(K_{DB1}K_{DB2})} \quad (1)$$

where A represents the radioligand (the dopamine D_1 receptor antagonist [^{3}H]SCH 23390 or the adenosine A_{2A} receptor antagonist [^{3}H]ZM 241385) concentration, R_T is the total amount of receptor dimers and K_{DA1} and K_{DA2} are the macroscopic dissociation constants describing the binding of the first and the second radioligand molecule (A) to the dimeric receptor; B represents the assayed competing compound (the dopamine D_1 receptor agonists SKF 81297 and SKF 38393 or the adenosine receptor agonist CGS 21680) concentration and K_{DB1} and K_{DB2} are, respectively, the equilibrium dissociation constants of the first and second binding of B; K_{DAB} can be described as a hybrid equilibrium radioligand/competitor dissociation constant, which is the dissociation constant of B binding to a receptor dimer semi-occupied by A.

Since the radioligand A (the antagonist [^{3}H]SCH 23390 or the antagonist [^{3}H]ZM 241385) showed non-cooperative behaviour ([1,19] and results not shown), Eq. (1) was simplified to Eq. (2) due to the fact that $K_{DA2} = 4K_{DA1}$ (see [19]):

$$A_{bound} = \frac{(4K_{DA1}A + 2A^2 + 4K_{DA1}AB/K_{DAB})R_T}{4K_{DA1}^2 + 4K_{DA1}A + A^2 + 4K_{DA1}AB/K_{DAB} + 4K_{DA1}^2B/K_{DB1} + 4K_{DA1}^2B^2/(K_{DB1}K_{DB2})} \quad (2)$$

The dimer cooperativity index for the competing ligand B (the agonists SKF 81297 or SKF 38393 for dopamine D_1 receptors, or the agonist CGS 21680 for adenosine A_{2A} receptors) was calculated as (see [19]):

$$D_{CB} = \log\left(\frac{4K_{DB1}}{K_{DB2}}\right) \quad (3)$$

A direct calculation of the concentration of B providing half saturation (B_{50}) was obtained according to Casadó et al. [19]:

$$B_{50} = (K_{DB1}K_{DB2})^{1/2} \quad (4)$$

In the experimental conditions when both the radioligand A (the antagonist [^{3}H]SCH 23390 or the antagonist [^{3}H]ZM 241385) and the competitor B (the agonists SKF 81297 and CGS21680) show non-cooperativity, it results that $K_{DA2} = 4K_{DA1}$ and $K_{DB2} = 4K_{DB1}$, and Eq. (1) was simplified to:

$$A_{bound} = \frac{(4K_{DA1}A + 2A^2 + 4K_{DA1}AB/K_{DAB})R_T}{4K_{DA1}^2 + 4K_{DA1}A + A^2 + 4K_{DA1}AB/K_{DAB} + 4K_{DA1}^2B/K_{DB1} + K_{DA1}^2B^2/K_{DB1}^2} \quad (5)$$

For comparison, data were also fitted to the classical one-site receptor model when monophasic competition curves were

observed and to the classical two-independent-site receptor models when biphasic competition curves were obtained, using respectively the equations:

$$A_{bound} = \frac{RIC_{50}}{IC_{50} + B} \quad (6)$$

$$A_{bound} = \frac{R_H IC_{50H}}{IC_{50H} + B} + \frac{R_L IC_{50L}}{IC_{50L} + B} \quad (7)$$

where R, R_H and R_L are the specific binding in the absence of competing ligand. IC_{50}, IC_{50H} and IC_{50L} of the B compound are related with the respective equilibrium dissociation constants K_D, K_{DH} and K_{DL} according with Cheng and Prusoff [25] equation:

$$IC_{50H} = K_{DH}(1 + A/K_{DA}) \qquad IC_{50L} = K_{DL}(1 + A/K_{DA}) \quad (8)$$

Goodness of fit was tested according to reduced χ^2 value given by the nonlinear regression program. The test of significance for two different model population variances was based upon the *F*-distribution (see [2] for details). Using this *F* test, a probability greater than 95% ($p < 0.05$) was considered the criterion to select a more complex model (cooperativity in Eq. (2) or two-sites in Eq. (7)) over the simplest one (non-cooperativity in Eq. (5) or one-site in Eq. (6)). In all cases, a probability of less than 70% ($p > 0.30$) resulted when one model was not significantly better than the other. Results are given as parameter values ± SEM of three independent experiments.

3. Results

3.1. Comparison of macroscopic dissociation constants for the agonist SKF 81297 binding to D_1 dopamine receptor calculated by using the two-state dimer receptor model or the two-independent-site model for monomeric receptors

Competition experiments were performed with a constant concentration of radiolabelled dopamine D_1 receptor antagonist [^{3}H]SCH 23390 (1.8 nM or 0.8 nM) and increasing concentrations of dopamine D_1 receptor agonist, SKF 81297, as described in Section 2. Binding data (Figs. 1 and 2) were fitted to equations

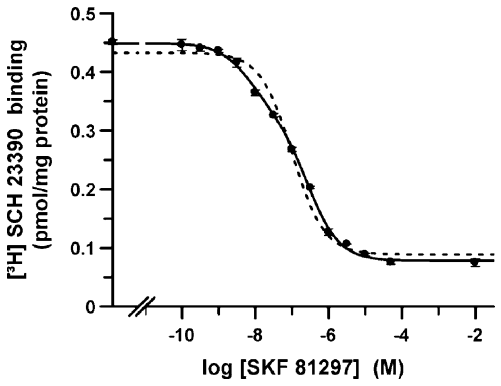

Fig. 1. Competition experiments using a relatively high D_1 receptor antagonist concentration versus increasing concentrations of the D_1 receptor agonist SKF 81297. Competition experiments of the D_1 receptor antagonist [^{3}H]SCH 23390 (1.8 nM) versus increasing concentrations of the D_1 receptor agonist SKF 81297 (0.1 nM to 50 μM) using sheep brain striatum membranes (0.5 mg protein/ml) were performed as indicated in Section 2. Binding data were fitted to the two-independent-site model (Eq. (7)) or to the two-state dimer receptor model (Eq. (5)) (solid line) and to the one-site receptor model (Eq. (6)) (dotted line). Using the *F* test, a probability greater than 95% ($p < 0.05$) was obtained to consider significant better the two-state dimer receptor model or the two-independent-site model over the one-site one. Data fit enough well to the two-state dimer receptor model (Eq. (5)) and no significant better fit was obtained considering Eq. (2). Mean ± SEM values from a representative experiment performed in triplicates are shown (see Supplementary material for sets of data points).

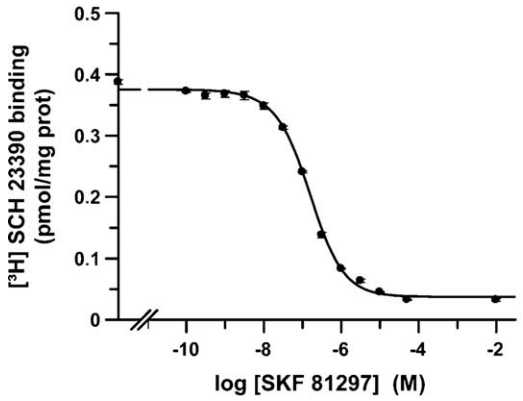

Fig. 2. Competition experiments using a relatively low D_1 receptor antagonist concentration versus increasing concentrations of the D_1 receptor agonist SKF 81297. Competition experiments of the D_1 receptor antagonist [^{3}H]SCH 23390 (0.8 nM) versus increasing concentrations of the D_1 receptor agonist SKF 81297 (0.1 nM to 50 μM) using sheep brain striatum membranes (0.5 mg protein/ml) were performed as indicated in Section 2. Binding data were fitted to the two-state dimer receptor model (Eq. (5)) or to the one-site receptor model (Eq. (6)). Using the *F* test, no significant better fit was obtained by considering more complex models (two-state dimer receptor model Eq. (2) or two independent-site receptor model Eq. (7)) over the simplest one. Mean ± SEM values from a representative experiment performed in triplicates are shown.

derived from the two-state dimer receptor model [1,19]. [^{3}H]SCH 23390 binding to D_1 receptor showed linear Scatchard plots [19]; thus, binding data were fitted to Eqs. (2) and (5) (see Section 2) introducing the previously reported K_{DA1} value of 0.47 nM for the non-cooperative [^{3}H]SCH 23390 binding to D_1 receptor [19]. At 1.8 nM [^{3}H]SCH 23390 a biphasic curve was obtained (Fig. 1) and the fit of the binding data to the Eq. (2) was not better than the fit to Eq. (5). In fact, binding data from competition curve fit enough well to the two-state dimer receptor model without cooperativity in SKF 81297 binding (solid line in Fig. 1) and the calculated values for parameters R_T, K_{DB1} and the hybrid parameter, K_{DAB} (see Section 2), are shown in Table 1. This hybrid parameter, K_{DAB}, which reflects an agonist–antagonist modulation, is instrumental to explain a biphasic curve by means of a non-cooperative binding (see Section 4). For comparative purposes, binding data were also fitted assuming one- or two-sites of monomeric receptors. Data from the biphasic curve was poorly handled by assuming one (monomeric) site and, therefore, binding data fit well to two sites (Fig. 1). Assuming momeric receptors monophasic curves are only explained by binding to one site whereas biphasic curves require two independent centers with significantly different equilibrium constant values. Fitting data to Eqs. (7) and (8) the two equilibrium constants were obtained (Table 1): R_H (high-affinity) and R_L (low-affinity), being approximately 35:65 the proportion of receptors in high-affinity (usually considered coupled to G-proteins) versus those in low-affinity (usually considered uncoupled to G-proteins). At 0.8 nM [^{3}H]SCH 23390 (Fig. 2) a monophasic competition curve was obtained. Binding data were fitted assuming the two-state dimer receptor model and also assuming one (Eq. (6)) or two (Eq. (7)) (monomeric) sites. Data shown in Fig. 2 fitted enough well to a dimer without cooperativity (Eq. (5)) and to one (monomeric) site (Eq. (6)) and no improvement was found by data fitting to a more complex equation (Eq. (7)). It should be noted that the parameters deduced using the two-state dimer receptor model (Table 1) are not significantly different from the ones obtained using a higher radioligand concentration, indicating that the two-state dimer receptor model is robustly giving consistent parameter values independently of the radioligand concentration used. On the contrary, parameter values calculated assuming monomers differ in the two experimental conditions (high versus low radioligand concentration; see Table 1).

Table 1
Parameter values obtained by fitting data from competition experiments of the antagonist [^{3}H]SCH 23390 binding to D_1 dopamine receptors with the agonist SKF 81297 to different models.

Model	Parameters	1.8 nM [^{3}H]SCH 23390	0.8 nM [^{3}H]SCH 23390
One-site receptor model	R (pmol/mg protein)		0.54 ± 0.07
	K_D (nM)		56 ± 8
Two-independent-site model	R_H (pmol/mg protein)	0.16 ± 0.02	
	K_{DH} (nM)	1.7 ± 0.4	
	R_L (pmol/mg protein)	0.30 ± 0.04	
	K_{DL} (nM)	62 ± 10	
Two-state dimer receptor model	R_T (pmol/mg protein)	0.34 ± 0.03	0.38 ± 0.03
	K_{DB1} (nM)	7 ± 2	6 ± 1
	K_{DB2} (nM)	28 ± 4	24 ± 5
	K_{DAB} (nM)	3 ± 1	1.5 ± 0.7
	D_{CB}	0	0
	D_{AB}	0.6 ± 0.1	0.8 ± 0.2
	B_{50} (nM)	14 ± 2	12 ± 2

Data are mean ± SEM values from three experiments. R is the maximum specific binding and K_D is the equilibrium dissociation constant for the competing ligand B (SKF 81297). R_H and R_L are, respectively, the maximum specific binding corresponding to, respectively, high- and low-affinity sites, and K_{DH} and K_{DL} are the equilibrium dissociation constants for, respectively, high- and low-affinity sites. R_T is the total amount of receptor dimers, K_{DB1} and K_{DB2} are, respectively, the equilibrium dissociation constants of the first and second binding of B to the dimer. K_{DAB} is the hybrid equilibrium dissociation constant of B binding to a receptor dimer semi-occupied by the A ([^{3}H]SCH 23390). D_{CB} is the dimer cooperativity index for the binding of ligand B and D_{AB} is the dimer radioligand/competitor modulation index. B_{50} is the concentration providing half saturation for B.

3.2. Useful new pharmacological parameters can be obtained from competition curves considering the two-state dimer receptor model

From the two-state dimer receptor model new parameters can be obtained that provide relevant and useful information. One of such parameters is the cooperative index (D_C). D_C would be a measure of the orthosteric dissociation equilibrium constant value modifications occurring when a protomer senses the binding of the same ligand molecule to the partner protomer (in a dimer). For the agonist SKF 81297 binding to D_1 receptors the D_C value was zero (D_{CB} in Table 1). A 0 value indicates that there is not any sign of cooperativity, i.e. the SKF 81297 binding to one protomer in the dimer did not modify the affinity for SKF 81297 in the other protomer in the dimer.

Another pharmacological parameter is the hybrid equilibrium dissociation constant (K_{DAB} in Eqs. (1), (2) and (5)). The K_{DAB} constant corresponds to the equilibrium dissociation constant for the competing ligand (B) when the dimer is semi-occupied by the radioligand (A). The value of K_{DAB} in Table 1 is the dissociation constant of the agonist SKF 81297 binding to a receptor dimer semi-occupied by the antagonist [^{3}H]SCH 23390. When $K_{DAB} = 2\ K_{DB1}$ the binding of the radioligand to one protomer in the dimer does not modify the binding of the competing ligand to the other empty protomer in the dimer. In contrast, values of $K_{DAB} < 2K_{DB1}$ or $K_{DAB} > 2K_{DB1}$ indicate, respectively, a positive or negative effect exerted by the radioligand on the competitor binding to the empty protomer (see Supplemental Material for details). This effect is exerted by ligand binding to one orthosteric site over the binding of a different ligand to the second orthosteric site in the dimer. This means that it is possible to measure whether the antagonist [^{3}H]SCH 23390 binding to a empty receptor dimer modulates (negatively or positively) the agonist SKF 81297 binding to the other subunit in the dimer. According to this, we here introduce a new parameter, "the dimer radioligand/competitor modulation index" (D_{AB}) ("SCH 23390/SKF 81297 modulation index", see Table 1) which is defined as $D_{AB} = \log(2\ K_{DB1}/K_{DAB})$. The way as the index is defined is such that its value is "0" when the radioligand binding to a protomer does not affect the competitor binding to the empty protomer in the dimer. Positive or negative values of D_{AB} indicate that the presence of a radioligand bound to a increases or decreases, respectively, the competitor affinity for binding to the empty protomer in the dimer. The $D_{AB} = 0.6$ for D_1 dopamine receptor described in Table 1 indicates positive modulation between [^{3}H]SCH 23390 and SKF 81297 binding.

Furthermore, from a pharmacological point of view, one interesting aspect of the two-state dimer receptor model is that it allows a direct calculation of the concentration providing half saturation for the tested compound (B_{50}) that corresponds exactly to the concentration of agonist providing half saturation for the competing ligand, independent of the biphasic or monophasic nature of the competition curve or of the radioligand concentration (see Table 1).

3.3. Pharmacological parameters for the agonist SKF 38393 binding to D_1 dopamine receptor calculated assuming dimers or monomers

Experiments at two different concentrations of the dopamine D_1 receptor antagonist [^{3}H]SCH 23390 (0.11 and 0.67 nM) were performed and the competition curve obtained increasing concentrations of the dopamine D_1 receptor agonist, SKF 38393, was biphasic in both cases (Fig. 3). Considering the two-state dimer receptor model, the fit of the binding data to Eq. (2) was better than the fit to Eq. (5). In fact, binding data fit well to the two-state dimer receptor model with cooperativity on the binding of SKF 38393 (solid line in Fig. 3A and B) and the calculated parameter values are shown in Table 2. Binding data were also fitted considering the one-site or two-independent-site monomeric receptor models. As it is shown in Fig. 3, binding data fit well to two (monomeric) sites or to a dimer. By fitting data to Eqs. (7) and (8), K_{DH} (high-affinity) and K_{DL} (low-affinity) equilibrium constants were obtained (Table 2). The parameters deduced using the two-state dimer receptor model are not significantly different using high or low radioligand concentrations, indicating that the two-state dimer receptor model is robust. On the contrary, parameter values for the high-affinity state calculated assuming monomers differ in the two experimental conditions (high versus low radioligand concentration; see Table 2).

3.4. Pharmacological parameters for the agonist CGS 21680 binding to A_{2A} adenosine receptor calculated assuming dimers or monomers

Competition experiments were performed at two different constant concentrations of the radiolabelled adenosine A_{2A} receptor antagonist [^{3}H]ZM-241385 (0.7 or 3.6 nM), and increasing concentrations of the adenosine A_{2A} receptor agonist, CGS 21680. Binding data (Fig. 4) were fitted to equations derived from the two-state dimer receptor model taking into account that [^{3}H]ZM-241385 binding to adenosine A_{2A} receptor shows linear Scatchard plots (results not shown). Therefore binding data must be fitted to Eqs. (2) and (5) by introducing the previously obtained K_{DA1} value of 0.66 nM. For both radioligand concentrations used, the fit of the binding data to the Eq. (2) was not better than the fit to Eq. (5) thus indicating that binding of CGS21680 is non-cooperative (solid line in Fig. 4A and B). Binding data were also fitted considering one or two sites. As it is shown in Fig. 4A, at the higher concentration binding data fit better to two than to one (monomeric) (Fig. 4A). In contrast, as shown in Fig. 4B, data obtained at low radioligand concentration fit fairly well to the equations describing binding to one site l (Eq. (6)) and no improvement was found using the

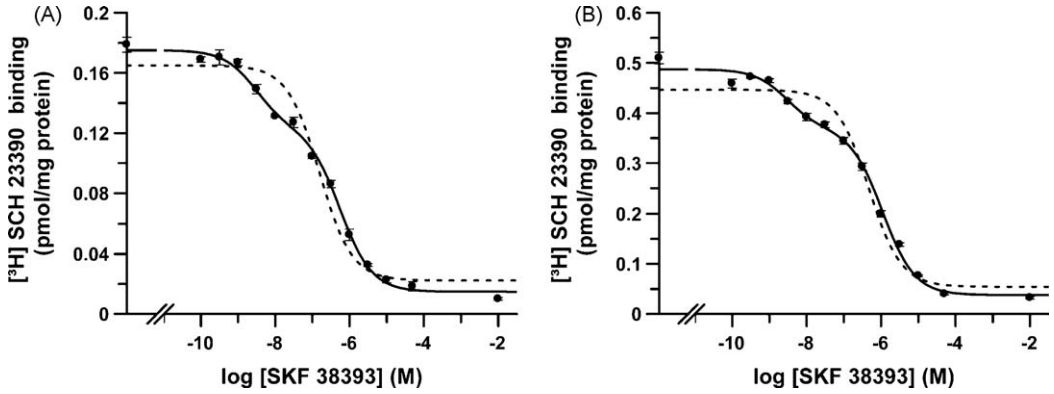

Fig. 3. Competition experiments using D_1 receptor antagonist versus increasing concentrations of the D_1 receptor agonist SKF 38393. Competition experiments of 0.11 nM (A) or 0.67 nM (B) D_1 receptor antagonist [^{3}H]SCH 23390 versus increasing concentrations of the D_1 receptor agonist SKF 38393 (0.1 nM to 50 μM) using sheep brain striatum membranes (0.27 mg protein/ml) were performed as indicated in Section 2. Binding data were fitted to the two-independent-site model (Eq. (7)) or to the two-state dimer receptor model (Eq. (2)) (solid line) and to the one-site receptor model (Eq. (6)) (dotted line). Using the *F* test, a probability greater than 95% ($p < 0.05$) was obtained to consider significant better the two-state dimer receptor model or the two-independent-site model over the one-site one. Mean ± SEM values from a representative experiment performed in triplicates are shown.

equation describing binding to two independent monomeric sites (Eq. (7)). The parameters deduced appear in Table 3.

4. Discussion

4.1. Useful new pharmacological parameters can be obtained from competition curves considering the two-state dimer receptor model

One interesting aspect of the two-state dimer receptor model is that the values of the different parameters can provide more information than those from the two-independent-site model. Using the two-state dimer receptor model the number of receptor dimers (R_T), which correspond to half of maximum binding, are directly obtained without any *a priori* assumption about coupling or uncoupling to G-proteins or else. The two macroscopic constants (K_{DB1} and K_{DB2}) correspond to the ligand binding to an empty dimer and to a semi-occupied dimer, respectively. Comparison of values in Tables 1–3 shows that the macroscopic constants, K_{DB1} and K_{DB2}, are different from the K_{DH} and K_{DL} obtained assuming the classical monomeric models. It should be noted that the difference is not only numerical but also conceptual; in fact, the meaning of K_{DB1} and K_{DB2} versus K_{DH} and K_{DL} is quite different and for a dimeric GPCR it is more straightforward to use K_{DB1} and K_{DB2}.

Table 2
Parameter values obtained by fitting data from competition experiments of the antagonist [^{3}H]SCH 23390 binding to D_1 dopamine receptors with the agonist SKF 38393.

Model	Parameters	0.67 nM [^{3}H]SCH 23390	0.11 nM [^{3}H]SCH 23390
Two-independent-site model	R_H (pmol/mg protein)	0.20 ± 0.01	0.32 ± 0.03
	K_{DH} (nM)	1.4 ± 0.3	4.6 ± 0.9
	R_L (pmol/mg protein)	0.56 ± 0.01	0.54 ± 0.03
	K_{DL} (nM)	540 ± 40	530 ± 90
Two-state dimer receptor model	R_T (pmol/mg protein)	0.47 ± 0.02	0.48 ± 0.03
	K_{DB1} (nM)	2.7 ± 0.7	2.7 ± 0.7
	K_{DB2} (nM)	330 ± 50	430 ± 50
	K_{DAB} (nM)	2.1 ± 0.6	3 ± 1
	D_{CB}	−1.5 ± 0.2	−1.6 ± 0.2
	D_{AB}	0.4 ± 0.2	0.2 ± 0.1
	B_{50} (nM)	30 ± 6	34 ± 6

Data are mean ± SEM values from three experiments. K_{DH} and K_{DL} are the equilibrium dissociation constants for, respectively, high- and low-affinity sites for the ligand B (SKF 38393). R_T is the total amount of receptor dimers, K_{DB1} and K_{DB2} are, respectively, the equilibrium dissociation constants of the first and second binding of B to the dimer. K_{DAB} is the hybrid equilibrium dissociation constant of B binding to a receptor dimer semi-occupied by the A ([^{3}H]SCH 23390). D_{CB} is the dimer cooperativity index for the binding of ligand B and D_{AB} is the dimer radioligand/competitor modulation index. B_{50} is the concentration providing half saturation for B.

For receptor homodimers, the binding of the first ligand to the orthosteric site in the dimer can modify the equilibrium parameters of the second ligand molecule binding to the other orthosteric site in the dimer and, in this case, cooperativity naturally comes from homotropic (the same ligand is modulating) ligand-driven intramolecular conformational changes in the dimer. In fact, one of the main advantages provided by the two-state dimer receptor model is the calculation of a cooperative index (D_C). D_C would be a measure of the orthosteric dissociation equilibrium constant value modifications occurring when a protomer senses the binding of the same ligand molecule to the partner protomer (in a dimer). Comparing the SKF 81297 and the SKF 38393 binding to dopamine D_1 receptors it was demonstrated that the homotropic cooperativity appearance depends on the characteristics of the ligand being used. In fact, the partial agonist SKF 38393 displayed negative homotropic cooperativity (negative D_{CB} value in Table 2). In contrast, for the full agonist, SKF 81297, binding to D_1 receptors the D_C value was zero (Table 1) indicating that there is not any sign of cooperativity, i.e. the SKF 81297 binding to one protomer in the dimer did not modify the affinity for SKF 81297 in the other protomer in the dimer. One interesting aspect that requires attention is that biphasic competition curves are usually interpreted by dimer models as resulting from negative cooperativity. It would seem therefore paradoxical to obtain a biphasic curve for non-cooperative binding to a receptor dimer (see Fig. 1 and Table 1). But this is indeed possible due to the fact that the one orthosteric ligand may affect the binding of a different orthosteric ligand. The hybrid equilibrium dissociation constant (K_{DAB}) is a measure of this ligand–ligand modulation. In fact, the K_{DAB} constant corresponds to the equilibrium dissociation constant for the competing ligand (B) when the dimer is semi-occupied by the radioligand (A). This means that it is possible to measure, by the dimer radioligand/competitor modulation index (D_{AB}), whether the antagonist [^{3}H]SCH 23390 binding to a empty receptor dimer modulates (negatively or positively) the agonist SKF 81297 binding to the other subunit in the dimer. When this type of modulation occurs, the competition curve shape depends not only on the homotropic cooperativity of the competitor (D_{CB}) but also on the radioligand/competitor modulation. This new concept of modulation between two different orthosteric ligands, i.e. antagonist/agonist, proves to be very useful when analysing competition

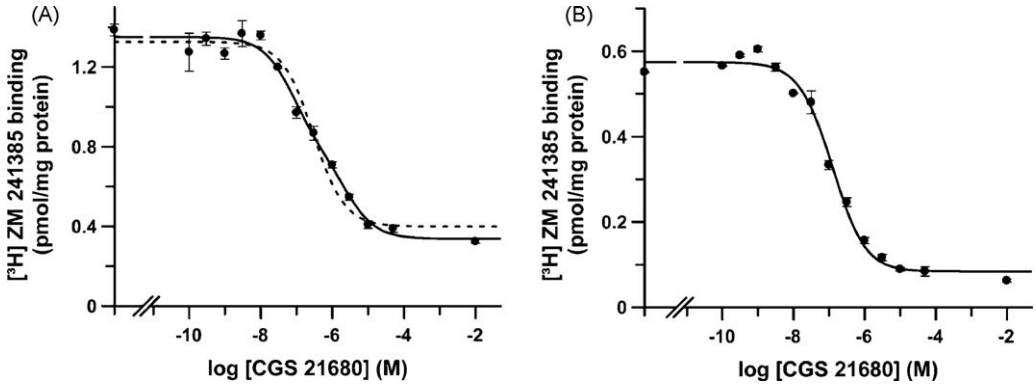

Fig. 4. Competition experiments using an adenosine A_{2A} receptor antagonist radioligand versus increasing concentrations of an adenosine A_{2A} receptor agonist. Competition experiments of the A_{2A} receptor antagonist [^{3}H]ZM-241385 (3.6 nM in A or 0.7 nM in B) versus increasing concentrations of the A_{2A} receptor agonist CGS 21680 (0.1 nM to 50 μM) using sheep brain striatum membranes (0.4 mg protein/ml) were performed as indicated in Section 2. In A, binding data were fitted to the two-independent-site model (Eq. (7)) or to the two-state dimer receptor model (Eq. (5)) (solid line) and to the one-site receptor model (Eq. (6)) (dotted line). Using the *F* test, a probability greater than 95% ($p < 0.05$) was obtained to consider significant better the two-state dimer receptor model or the two-independent-site model over the one-site one. Data fit enough well to the two-state dimer receptor model (Eq. (5)) and no significant better fit was obtained considering Eq. (2). In B, binding data were fitted to the two-state dimer receptor model (Eq. (5)) or to the one-site receptor model (Eq. (6)). Using the *F* test, no significant better fit was obtained by considering more complex models (two-state dimer receptor model Eq. (2) or two independent-site receptor model Eq. (7)) over the simplest one. Mean ± SEM values from a representative experiment performed in triplicates are shown.

experiments. The D_{AB} for D_1 dopamine receptor described in Table 1 indicates positive modulation between [^{3}H]SCH 23390 and SKF 81297 binding that induces the appearance of a biphasic competition curve even in the absence of any homotropic cooperativity. This phenomenon was further illustrated by the simulation curves displayed in Fig. 5. Assuming that there is a marked positive modulation between the radioligand and the competing ligand, the two-state dimer receptor model predicts the evolution from biphasic competition curves to monophasic ones when decreasing the radioligand concentration (Fig. 5). This was proved by competition experiments with a relatively low radioligand antagonist concentration to diminish the effect of antagonist/agonist modulation according to the prediction shown in Fig. 5. For the low radioligand concentration, the parameters deduced for SKF 81297 binding to D_1 dopamine receptor, using the two-state dimer receptor model (Table 1) are not significantly different from the ones obtained using higher radioligand concentration, indicating that the two-state dimer receptor model is robustly giving consistent parameter values independently of the radioligand concentration used. On the contrary, the parameters deduced from a monomer-based model differ in the two experimental conditions and, since this is not possible under a mechanistic point of view, this indicates that the monomer-based model is unable to explain the experimental results. One interesting feature arises when comparing values of pharmacological parameters obtained using the two-state dimer receptor model for the two different radioligand concentrations used (Table 1, Figs. 1 and 2). In fact, the experimental results demonstrate that the antagonist/agonist modulation induces, at high antagonist concentrations, the appearance of a

Table 3
Parameter values obtained by fitting data from competition experiments of the antagonist [^{3}H]ZM-241385 binding to adenosine A_{2A} receptors with the agonist CGS 21680 to different models.

Model	Parameters	3.6 nM [^{3}H]ZM-241385	0.7 nM [^{3}H]ZM-241385
One-site receptor model	R (pmol/mg protein)		0.9 ± 0.02
	K_D (nM)		56 ± 5
Two-independent-site model	R_H (pmol/mg protein)	0.7 ± 0.1	
	K_{DH} (nM)	11 ± 4	
	R_L (pmol/mg protein)	0.5 ± 0.1	
	K_{DL} (nM)	340 ± 140	
Two-state dimer receptor model	R_T (pmol/mg protein)	0.68 ± 0.02	0.70 ± 0.01
	K_{DB1} (nM)	31 ± 5	24 ± 6
	K_{DB2} (nM)	124 ± 20	96 ± 24
	K_{DAB} (nM)	20 ± 6	27 ± 8
	D_{CB}	0	0
	D_{AB}	0.5 ± 0.2	0.3 ± 0.2
	B_{50} (nM)	60 ± 10	50 ± 10

Data are mean ± SEM values of three experiments. R is the maximum specific binding and K_D is the equilibrium dissociation constant for the competing ligand B (CGS 21680). R_H and R_L are, respectively, the maximum specific binding corresponding to, respectively, high- and low-affinity sites, and K_{DH} and K_{DL} are the equilibrium dissociation constants for, respectively, high- and low-affinity sites. R_T is the total amount of receptor dimers, K_{DB1} and K_{DB2} are, respectively, the equilibrium dissociation constants of the first and second binding of B to the dimer. K_{DAB} is the hybrid equilibrium dissociation constant of B binding to a receptor dimer semi-occupied by the A ([^{3}H]ZM-241385). D_{CB} is the dimer cooperativity index for the binding of ligand B and D_{AB} is the dimer radioligand/competitor modulation index. B_{50} is the concentration providing half saturation for B.

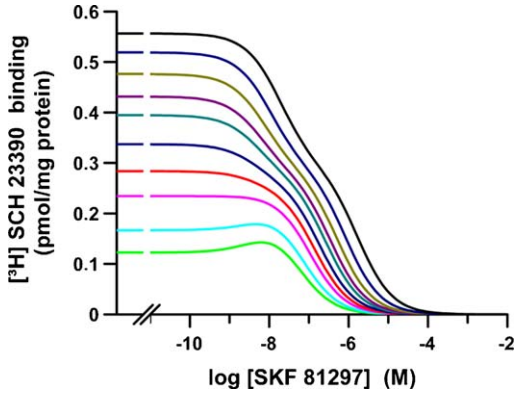

Fig. 5. Competition curves simulation. Simulation was performed considering the Eq. (2) and the following parameter values: R_T = 0.3 (pmol/mg protein), K_{DA1} = 0.47 nM, K_{DB1} = 6.5 nM, K_{DB2} = 26 nM, K_{DAB} = 2.5 nM, using different radioligand concentrations (A in Eq. (2); 0.1, 0.2, 0.3, 0.5, 0.7, 1.0, 1.5, 2.0, 3.0, 5.0 and 10 nM bottom to top) and increasing concentrations of the D_1 receptor agonist (B in Eq. (2); 0.001 nM to 1 mM).

biphasic competition curve, independent of the existence or not of competitor homotropic cooperativity as predicted by the two-state dimer receptor model.

To extend this conclusion beyond dopamine receptors, agonist versus antagonist competition experiments of binding to adenosine A_{2A} receptors were performed at two different radioligand concentrations (Fig. 4). The parameters deduced using the two-state dimer receptor model, but not those deduced from a monomer-based model (Table 3), were similar at low or high radioligand concentrations, indicating that the two-state dimer receptor model is robustly giving consistent parameter values. For the agonist, CGS 21680, binding to adenosine A_{2A} receptors the D_{CB} value was zero (Table 3) indicating that there is not any sign of cooperativity, i.e. the CGS 21680 binding to one protomer in the dimer did not modify the affinity for CGS 21680 binding to the other protomer in the dimer. This is another model system in which a biphasic curve results from non-cooperative binding to a receptor dimer (see Fig. 1 and Table 1). Again, this is feasible due to the fact that the one orthosteric ligand affects the binding of a different orthosteric ligand, something that may be quantitated in the form of a hybrid equilibrium dissociation constant (K_{DAB}). A radioligand/competitor modulation index (D_{AB}) of approximately 0.4 for A_{2A} receptor was calculated indicating positive modulation between [^{3}H]ZM-241385 and CGS 21680 binding that induces the appearance of a biphasic competition curve even in the absence of any homotropic cooperativity. Collectively, the results indicate that the two-state dimer receptor model is a suitable model to handle binding data to GPCRs.

4.2. Monomeric models cannot handle changes in the proportion of low- and high-affinity sites induced by varying the radioligand concentration

Since the two-independent-site model assumes that the states are independent and not modified by the ligands, the significant changes in the proportion of low- and high-affinity sites induced by varying the radioligand concentration (see Tables 1–3) cannot be explained using such a model. At low radioligand concentration the proportion of receptors in high-affinity (usually considered coupled to G-proteins) versus those in low-affinity (usually considered uncoupled to G-proteins) was 0:100 for SKF 81297 or 37:63 for SKF 38393 binding to dopamine D_1 receptors whereas they were 35:65 and 26:74, respectively, at the higher radioligand concentration. For the CGS 21860 binding to adenosine A_{2A} receptors this proportion at low radioligand concentration was 0:100 whereas it was 58:42 at the higher radioligand concentration. These data are inconsistent, which proves that the monomeric model cannot handle such experimental data. Using the two-state dimer receptor model the number of receptor dimers (R_T), which correspond to half of maximum binding, are directly obtained without any *a priori* assumption about coupling or uncoupling to G-proteins or else.

4.3. Can high- and low-affinity constants to receptor dimers be calculated from competition experiments?

Scientists usually use the two-independent-site monomeric model to fit pharmacological data and drug screening is usually performed by means of radioligand antagonist/drug competition curves from which high- (K_{DH}) and low (K_{DL})-affinity (equilibrium) constants are calculated.

As described in this paper the meaning and in some cases (as for SKF81297 binding to D_1 dopamine receptors or CGS 21860 binding to A_{2A} adenosine receptors) the existence of these two receptor affinity sites apparently depends upon the concentration of the radioligand. Moreover, it may happen that at relatively high radiolabelled antagonist concentrations, the percentage of receptors showing high-affinity for the agonist is different from that obtained performing the experiment at relatively low radiolabelled antagonist concentration (Tables 1–3). Since the two-independent-site model assumes that the states are independent and not modified by the ligands, changes in the proportion of low- and high-affinity sites induced by varying the radioligand concentration in a competition experiment cannot be explained using such a model. Furthermore, none of the reported monomer-based models are able to explain the above-described results. In summary, one must be cautious when using classical (monomeric) models when trying to interpret biphasic competition curves. In sharp contrast, the two-state dimer receptor model predicts at low radioligand concentrations the "disappearance" of one affinity state (Tables 1 and 3) as a consequence of a radioligand/competitor modulation. This indeed constitutes one of the most interesting messages provided herewith, i.e. a direct translation of a biphasic competition curve into the existence of two affinity sites or into the existence of homotropic cooperativity of the competitor may not be correct.

At the two radiolabelled antagonist concentrations assayed, the macroscopic parameters, i.e. the equilibrium constants, obtained using the two-state dimer receptor model (Tables 1–3) are similar and are independent of the monophasic or the biphasic nature of the competition curve. This may be considered a proof of the usefulness of the model since the concentration of the radioligand should not modify the values of the parameters. Furthermore, from a pharmacological point of view, one interesting aspect of the two-state dimer receptor model is that it allows a direct calculation of the concentration providing half saturation for the tested compound (B_{50}). As demonstrated here, the parameter, B_{50}, is more suitable than the usually employed IC_{50} values for ordering the compounds according to their binding potency. For dopamine D_1 receptor and adenosine A_{2A} receptor the B_{50} calculated using Eq. (4) and reported in Tables 1–3 corresponds to the concentration of agonist providing half saturation for the competing ligand, independent of the biphasic or monophasic nature of the competition curve or of the radioligand concentration. In contrast, the two IC_{50} values, obtained using the classical monomer-based receptor model, have an ambiguous meaning. IC_{50} values depend on the radioligand concentration and on the shape of the curve (Fig. 2). Thus, is then evident that IC_{50} is not a useful parameter to use in cases of complex binding data.

Taking all these data into consideration, the two-state dimer receptor model gives information of maximum binding ($2R_T$), of macroscopic dissociation constants and moreover, relevant information about the existence and quantification of homotropic cooperativity (D_C) and radioligand/competitor affinity modulation (D_{AB}) and a reliable B_{50} value for ordering compounds according to their binding potency. In cases in which homotropic cooperativity or radioligand/competitor interaction exists, the two-state dimer model is the model of election to calculate macroscopic dissociation constants. This is of particular importance for pharmacologists to overcome drawbacks derived from the use of classical monomeric receptor models to fit binding data.

Acknowledgments

We acknowledge the technical help obtained from Jasmina Jiménez (Molecular Neurobiology laboratory, Fac. Biology, Barcelona University). This study was supported by Grants from Spanish Ministerio de Ciencia y Tecnología (SAF2005-00170 and SAF2008-00146 to E.I.C. SAF2006-05481 to R.F.), grant 060110 from Fundació La Marató de TV3 to E.I.C.

Appendix A. Supplementary data

Supplementary data associated with this article can be found, in the online version, at doi:10.1016/j.bcp.2009.07.012.

References

[1] Franco R, Casadó V, Mallol J, Ferrada C, Ferré S, Fuxe K, et al. The two-state dimer receptor model: a general model for receptor dimers. Mol Pharmacol 2006;69:1905–12.

[2] Casadó V, Cantí C, Mallol J, Canela EI, Lluís C, Franco R. Solubilization of A_1 adenosine receptor from pig brain: characterization and evidence of the role of the cell membrane on the coexistence of high- and low-affinity states. J Neurosci Res 1990;26:461–73.

[3] Whorton MR, Bokoch MP, Rasmussen SG, Huang B, Zare RN, Kobilka B, et al. A monomeric G protein-coupled receptor isolated in a high-density lipoprotein particle efficiently activates its G protein. Proc Natl Acad Sci USA 2007;104:7682–7.

[4] Bouvier M. Oligomerization of G-protein-coupled transmitter receptors. Nat Rev Neurosci 2001;2:274–86.

[5] Devi LA. Heterodimerization of G-protein-coupled receptors: pharmacology, signaling and trafficking. Trends Pharmacol Sci 2001;22:532–7.

[6] Rios CD, Jordan BA, Gomes I, Devi LA. G-protein-coupled receptor dimerization: modulation of receptor function. Pharmacol Ther 2001;92:71–87.

[7] George SR, O'Dowd BF, Lee SP. G-protein-coupled receptor oligomerization and its potential for drug discovery. Nat Rev Drug Discov 2002;1:808–20.

[8] Agnati LF, Ferré S, Lluís C, Franco R, Fuxe K. Molecular mechanisms and therapeutical implications of intramembrane receptor/receptor interactions among heptahelical receptors with examples from the striatopallidal GABA neurons. Pharmacol Rev 2003;55:509–50.

[9] Agnati LF, Fuxe K, Ferré S. How receptor mosaics decode transmitter signals. Possible relevance of cooperativity. Trends Biochem Sci 2005;30:188–93.

[10] Franco R, Canals M, Marcellino D, Ferré S, Agnati L, Mallol J, et al. Regulation of heptaspanning-membrane-receptor function by dimerization and clustering. Trends Biochem Sci 2003;28:238–43.

[11] Franco R, Casadó V, Cortés A, Mallol J, Ciruela F, Ferré S, et al. G-protein-coupled receptors heteromers: function and ligand pharmacology. Br J Pharmacol 2008;153:S90–8.

[12] Terrillon S, Bouvier M. Roles of G-protein-coupled receptor dimerization. EMBO Rep 2004;5:30–4.

[13] Prinster SC, Hague C, Hall RA. Heterodimerization of G protein-coupled receptors: specificity and functional significance. Pharmacol Rev 2005;57:289–98.

[14] Milligan G. G-protein-coupled receptor heterodimers: pharmacology, function and relevance to drug discovery. Drug Discov Today 2006;11:541–9.

[15] Maurel D, Comps-Agrar L, Brock C, Rives ML, Bourrier E, Ayoub MA, et al. Cell-surface protein–protein interaction analysis with time-resolved FRET and snap-tag technologies: application to GPCR oligomerization. Nat Methods 2008;5:561–7.

[16] Franco R, Casadó V, Ciruela F, Mallol J, Lluis C, Canela EI. The cluster-arranged cooperative model: a model that accounts for the kinetics of binding to A1 adenosine receptors. Biochemistry 1996;5:3007–15.

[17] Franco R, Casadó V, Mallol J, Ferré S, Fuxe K, Cortés A, et al. Dimer-based model for heptaspanning membrane receptors. Trends Biochem Sci 2005;30:360–6.

[18] Durroux T. Principles: a model for the allosteric interactions between ligand binding sites within a dimeric GPCR. Trends Pharmacol Sci 2005;26:376–84.

[19] Casadó V, Cortés A, Ciruela F, Mallol J, Ferré S, Lluís C, et al. Old and new ways to calculate the affinity of agonists and antagonists interacting with G-protein-coupled monomeric and dimeric receptors: the receptor-dimer cooperativity index. Pharmacol Ther 2007;116:343–54.

[20] George SR, Lee SP, Varghese G, Zeman PR, Seeman P, Ng GY, et al. A transmembrane domain-derived peptide inhibits D1 dopamine receptor function without affecting receptor oligomerization. J Biol Chem 1998;273:30244–8.

[21] O'Dowd BF, Ji X, Alijaniaram M, Rajaram KD, Kong MM, Rashid A, et al. Dopamine receptor oligomerization visualized in living cells. J Biol Chem 2005;280:37225–3.

[22] Kong MM, Fan T, Varghese G, O'Dowd BF, George SR. Agonist-induced cell surface trafficking of an intracellularly sequestered D1 dopamine receptor homo-oligomer. Mol Pharmacol 2006;70:78–89.

[23] Canals M, Burgueño J, Marcellino D, Cabello N, Canela EI, Mallol J, et al. Homodimerization of adenosine A2A receptors: qualitative and quantitative assessment by fluorescence and bioluminescence energy transfer. J Neurochem 2004;88:726–34.

[24] Sarrió S, Casadó V, Escriche M, Ciruela F, Mallol J, Canela EI, et al. The heat shock cognate protein hsc73 assembles with A(1) adenosine receptors to form functional modules in the cell membrane. Mol Cell Biol 2000;20:5164–74.

[25] Cheng YC, Prusoff WH. Relationship between the inhibition constant (Ki) and the concentration of inhibitor which causes 50 percent inhibition (I_{50}) of an enzymatic reaction. Biochem Pharmacol 1973;22:3099–108.